The 2013 World Congress on
Advances in Structural Engineering and Mechanics (ASEM13)
Jeju, Korea, September 8-12, 2013

The Empirical Corner Stiffness for Right-angle Frames of Rectangular and H-type Cross-sections

*Young-Doo Kwon[1)], Soon-Bum Kwon[1)], Hyuck-Moon Gil[2)], Hee-Jeong Cho[3)]

[1)] School of Mechanical Engineering & IEDT, Kyungpook National University, Daegu, Korea
[2)] Department of Offshore Structure Design & Engineering, Hyundai Heavy Industry, Ulsan, Korea
[3)] Graduate School, Kyungpook National University, Daegu, Korea
** ydkwon@knu.ac.kr*

Abstract

The consistent growth of industry and improvements in living standards has placed continuous new demands on the water supply. Many dams have been constructed to meet these demands. A key component of a dam is the gates used to control and adjust the water levels and flow rates. A slide gate is typically used as a small-sized gate. Although its operating resistance is large, it has a simple structure and is relatively inexpensive. The role of the bonnet has been highlighted in high pressure slide gates. Until now, the finite corner stiffness of the right frames used as horizontal girders in a bonnet have not been considered during the design process, meaning that the current design concept for the girders in slide gates is not precise.

Accordingly, this paper presents design equation set I for the right frames used as horizontal girders in a bonnet, assuming rigid corner stiffness. By comparing the center stresses of the right frame using design equation set I with the result of FEM, the master curves for empirical corner stiffness could be determined as a function of slenderness ratio. The design equation set II for the right frame assuming finite corner stiffness was derived and compared with the former equations. Using the master curves for the corner stiffness and design equation set II, the precise design moments at the centers of the girder can be determined so the bending stresses can be analyzed more precisely. Therefore, when designing a right angle frame itself or right frames used as horizontal girders in the bonnet of a slide gate, the master curves for the corner stiffness can be used for a more precise analysis and design.

1. Introduction

The consistent growth of industry and improvements in living standards has placed new demands on the water supply. In particular, large barrages for constructing dams, a number of km in length, are being operated for balanced national development and the efficient use of water resources in many countries (Shariatmadar 2011).

[1)] Professor
[2) 3)] Graduate Student
Note: Copied from the manuscript submitted to "Structural Engineering and Mechanics, An International Journal" for presentation at ASEM13 Congress

A key component of a dam is the gate used to control the flow rates and adjust the water level. Many types of gates with their own characteristics have been developed. The slide gate is used typically as a small-sized gate. Although its operating resistance is large, it has a simple structure and its installation cost is relatively low (Lewin 2001, Hydraulic and Penstock Association1986)

The high pressure gate appeared with the successful application of the jet flow gate at Shasta dam in the 1940's, and many similar types have been attempted by the U.S. Army Corps of Engineers. Similar structures include the ring follower gate, jet flow gate and roller gate (Kwon 2000, Kwon 2004). These gates all have the structure of a bonnet wrapping around the gate. The bonnet of the slide gates is loaded by the inner high water pressure. Although an evaluation of an accurate corner moment is very important, the current design concept for the bonnet in a slide gate is inadequate based on the infinite corner stiffness (Timoshenko and Goodier 1970, Reismann and Pawlik 1980, Ugural and Fenster 2003)

This study proposes the empirical corner stiffness in the form of master curves that can be used with the theory developed based on the assumption of finite stiffness (Kwon 2013). The empirical corner stiffness was evaluated reversely from the deviation of stresses obtained assuming infinite corner stiffness and by the FEM. The accuracy of the new procedure for stress analysis of a right-angle frame was tested and confirmed by comparing the resulting stresses with the FEM results. Therefore, the proposed master curves for the empirical corner stiffness can be applied successively in the analysis and design of a right-angle frame with the referred theory of the finite corner stiffness.

2. Structure of the bonnet and design equations for right-angle frames

A bonnet is used in the high pressure slide gate installed deep under water to resist the high water pressures, and is composed of skins and horizontal girders with the shape of a right-angle frame. In designing the right frames, the stiffness of the corner is assumed to be rigid and the corresponding corner moment was confirmed based on that assumption. Using this corner moment, the center moments were calculated to evaluate the maximum bending stresses.

On the other hand, these stresses sometimes deviate considerably from the FEA. After an extensive trial and error process, the deviation of the results seems to be rooted in the inaccurate assumption of infinite corner stiffness. To resolve this problem, the finite corner stiffness was evaluated empirically based on the deviation of stresses. For a given cross-section of the right frame, a master curve could be obtained as a function of the slenderness ratio, regardless of the each dimension. More accurate center moments of the right frame and the corresponding accurate stresses could be obtained using this corner stiffness and referred design equation assuming finite corner stiffness.

2.1. Structure of the bonnet

Fig. 1 shows the entire bonnet structure of a high-pressure slide gate. The role of the gate is to allow or prevent water flow through up and down motion, and

the bonnet wraps around this gate. The bonnet structure consists of skin palates, and horizontal and vertical guides stiffness (Orbanich and Ortega 2013). This structure should be able to support hoisting loads as well as the inner water pressure. The horizontal girder is the structure stacked by a number of wide flanges, as shown in Fig. 2. Fig. 3 shows the side and top view of the bonnet structure, where c is the repeated height of the horizontal girder. The design of a wide flange beam with the proper width of the base flange is defined in reference (DIN 1976). As shown in Fig. 3 (b), L (section 2-3) and H (section 1-3), respectively, represent the each directional half-length of an inner side wall loaded water pressure directly. Similarly, L_1 and H_1 represent the length of a rectangular line passing through the centroid of the cross-section area of the horizontal girder.

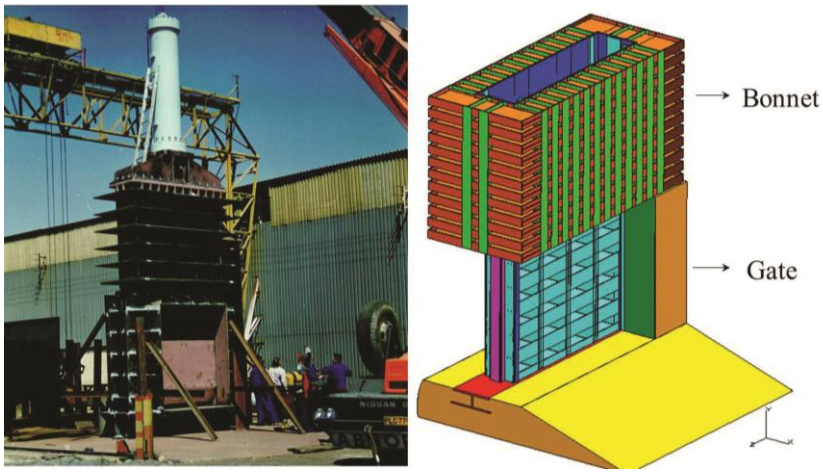

Fig.1 High pressure slide gate system

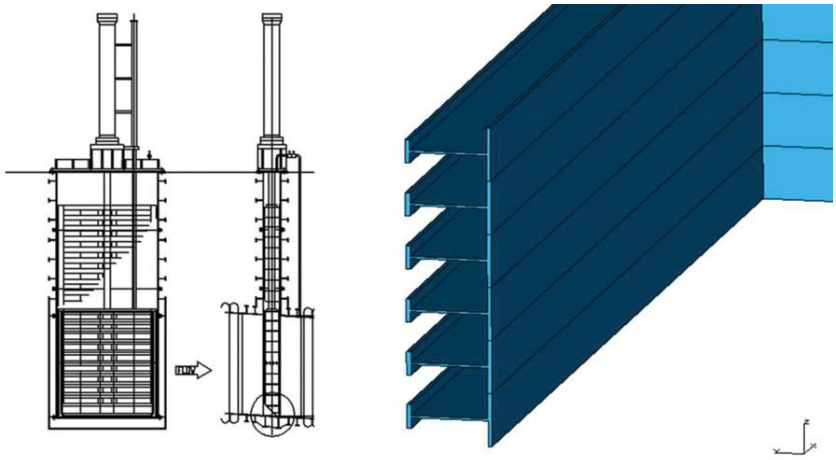

Fig. 2 Detailed view of the bonnet structure

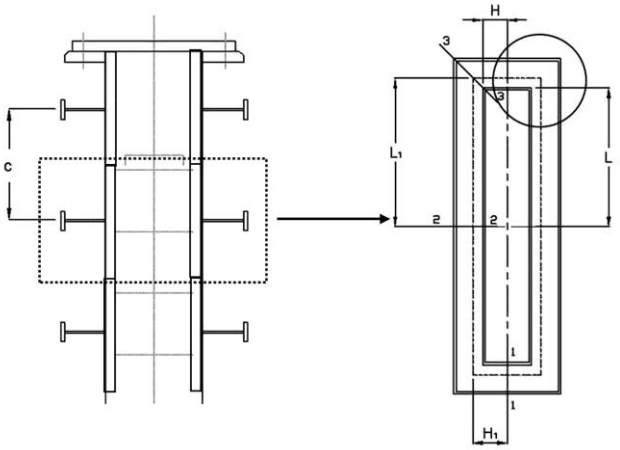

Fig. 3 Side view and top view of the bonnet with horizontal girders

2.2. Governing equation of the corner moment for the right-angle frames

In this paper, the governing equations were derived considering the stiffness of the corner part to infinity. This result was compared with that of FE analysis to evaluate the errors caused by the assumption. From these empirical errors, the actual corner stiffness could be evaluated by reverse computation. The corner stiffness for different sizes of a cross-section of the frame can be represented with a single master curve for a specific type of cross-section. The accurate design moments at the centers of the frame can be evaluated using this corner stiffness and the referred design equation considering the finite corner stiffness.

Consider a right-angle frame, which is a quarter model of the bonnet structure, as shown in Fig. 4, and is a typical formulation to analyze the conventional bonnet corner part of a slide gate. To simplify the problem, the corner stiffness was assumed to be infinite. The inner pressure P was converted to P_H, which is the redistributed load to the neutral plane of the horizontal girder's cross-section area, which can be written as

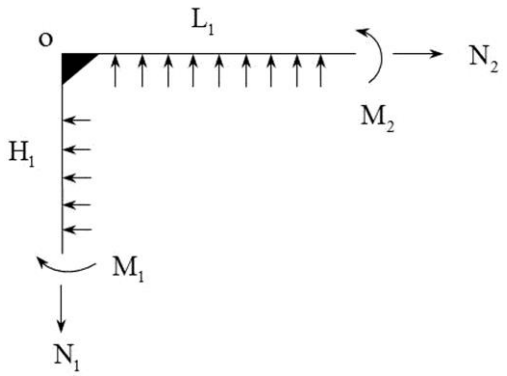

Fig. 4 Free body diagram quarter part of a horizontal girder with a rigid corner

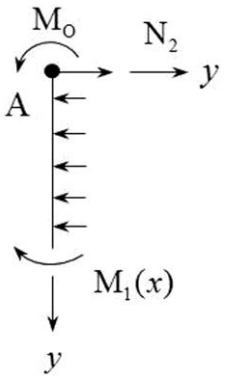

Fig. 5 FBD of section 1-3

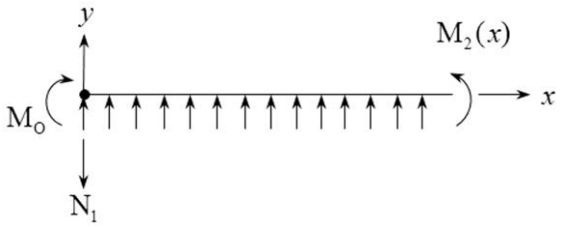

Fig. 6 FBD of section 2-3

$$P_H = P \times \frac{L+H}{L_1+H_1} \tag{1}$$

The intensity of load per unit length can be expressed as

$$Q_H = P_H \times c \tag{2}$$

The tensile loads N_1 and N_2 can be expressed as,

$$N_1 = Q_H \times L_1 \tag{3}$$

$$N_2 = Q_H \times H_1 \tag{4}$$

The right-angle frame model can be divided into two sections, as shown in Fig. 5 and 6 to show the Free Body Diagrams. The bending moment in section 1-3 at point x from o can be obtained by the moment equilibrium, which can be expressed as

$$M_1(x) = M_O + \frac{1}{2}Q_H x^2 - N_2 x \tag{5}$$

The differential equation for deflection curve is

$$w'' = -\frac{M_1}{EI} \tag{6}$$

where, w means the vertical deflection to the section beam. The gradient of deflection can be obtained by integrating Eq. (6), which can be written as

$$w' = \frac{1}{EI}(-M_O x - \frac{1}{6}Q_H x^3 + \frac{1}{2}N_2 x) + C_1 \tag{7}$$

The boundary conditions of the vertical section of the beam are

$$w'(0) = \theta_A \tag{8}$$

$$w'(H_1) = 0 \tag{9}$$

where, θ_A means the deflection angle at point A. By applying these boundary conditions to Eq. (7), the following equation should be satisfied:

$$0 = -M_O H_1 - \frac{1}{6} Q_H H_1^3 + \frac{1}{2} N_2 H_1^2 + \theta_A EI \tag{10}$$

Similarly, the bending moment in section 2-3 at point x from o can be obtained from

$$M_2(x) = M_O + \frac{1}{2} Q_H x^2 - N_1 x \tag{11}$$

The differential equation for deflection curve is expressed as Eq. (12), where the sign of the right hand term changes from negative in Eq. (6) to positive. The reason for this is that a different sign of moment was used for each section for the purpose of overall consistency of the sign of the moments in the entire structure. The deflection angle, Eq.(13), was obtained by substituting Eq. (11) into Eq. (12).

$$w'' = \frac{M_2}{EI} \tag{12}$$

$$w' = \frac{1}{EI}(M_O x + \frac{1}{6} Q_H x^3 - \frac{1}{2} N_1 x^2) + C_2 \tag{13}$$

where θ_B is the deflection angle at point B. After applying the boundary conditions,

$$w'(0) = \theta_B \tag{14}$$

$$w'(L_1) = 0\,, \tag{15}$$

to Eq. (13), Eq.(16) needs to be satisfied.

$$0 = M_O L_1 + \frac{1}{6} Q_H L_1^3 - \frac{1}{2} N_1 L_1^2 + \theta_B EI \tag{16}$$

From the condition of infinite corner rigidity, Eq. (17)

$$\theta_A = \theta_B\,, \tag{17}$$

needs to be satisfied, from which the corner moment, M_O, can be obtained based on the assumption of infinite corner stiffness as follows:

$$M_O = \frac{Q_H(L_1^3 + H_1^3)}{3(L_1 + H_1)} \tag{18}$$

The design equation set I for the moments at the centers of the frame can be expressed as Eqs. (19) and (20).

$$\begin{aligned} M_1(H_1) &= M_O + \frac{1}{2}Q_H H_1^{\,2} - N_2 H_1 \\ &= \frac{Q_H(L_1^3 + H_1^3)}{3(L_1 + H_1)} - \frac{1}{2}Q_H H_1^2 \end{aligned} \tag{19}$$

$$\begin{aligned} M_2(L_2) &= M_O + \frac{1}{2}Q_H L_1^{\,2} - N_2 L_1 \\ &= \frac{Q_H(L_1^3 + H_1^3)}{3(L_1 + H_1)} - \frac{1}{2}Q_H L_1^2 \end{aligned} \tag{20}$$

Therefore, when the corner stiffness is assumed to be infinite as a rigid corner, the analysis has been done and used in the design of the right-angle frames.

Here, refer to the extension for the case of finite corner stiffness of K_C. The formula for the corner moment, M_C, can be expressed as (Kwon 2013),

$$M_C = \frac{Q_H(L_1^3 + H_1^3)}{3(L_1 + H_1) + 3EI / K_C} \quad , \tag{21}$$

$M_1(H_1)$ and $M_2(L_1)$ in design equation set I need to be changed by replacing M_O with M_C, where M_C converges to M_O if the K_C approaches infinity. Design equation set II for the moments at the centers of the frame assuming finite corner stiffness can be expressed as Eqs. (22) and (23).

$$\begin{aligned} M_1(H_1) &= M_C + \frac{1}{2}Q_H H_1^{\,2} - N_2 H_1 \\ &= \frac{Q_H(L_1^3 + H_1^3)}{3(L_1 + H_1) + 3EI / K_C} - \frac{1}{2}Q_H H_1^2 \end{aligned} \tag{22}$$

$$\begin{aligned} M_2(L_2) &= M_C + \frac{1}{2}Q_H L_1^{\,2} - N_2 L_1 \\ &= \frac{Q_H(L_1^3 + H_1^3)}{3(L_1 + H_1) + 3EI / K_C} - \frac{1}{2}Q_H L_1^2 \end{aligned} \tag{23}$$

3. Comparison between the equation of K – M and the FEM result

Fig.7 shows the FE model, which is composed of many beam elements. The commercial program, NISA II(EMRC 1994), was used to solve the linear static problem under internal pressure. Table 1 lists the properties of this model. A torsion spring was applied to the corner connecting two beams simulating the corner stiffness of the right frame. Fig. 8 compares the two results, one is the theoretical result by Equation (21) of the K_C-M_C relation, and the other is the result of FEA with a torsional spring. As shown in the graph, the theoretical result is consistent with FEA, which means that the equation of the K_C-M_C relation has the precise validity. When the torsion stiffness, K_C, is infinitely large (Fig. 8), the corner moment can be observed, and M_C converges to the M_O = 1.5 x 10^7 N-mm.

Up to now, the corner stiffness was typically assumed to be infinite and has been used to calculate the corner moment and following design moments as in design equation set I. On the other hand, without an evaluation of the accurate corner stiffness, one cannot obtain the correct corner moment and the following design moments at the centers of the frame in design equation set II.

Table 1 Geometry, material properties and applied pressure

L_1 (mm)	1500	H_1 (mm)	1500
a (mm)	150	c = b (mm)	20
E (GPa)	207	ν	0.3
P (MPa)	1	I (mm^4)	5,625,000

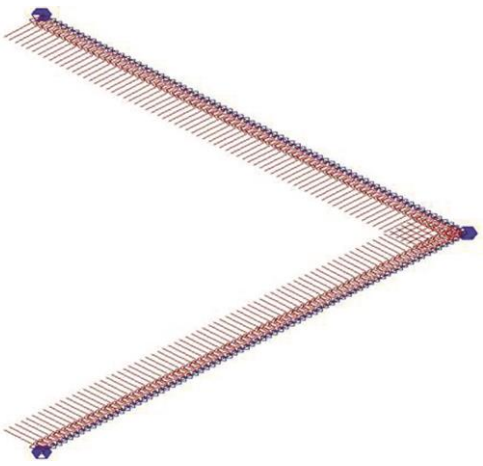

Fig. 7 Finite element beam model of the horizontal girder with the corner torsional spring of stiffness K_C using NISA II

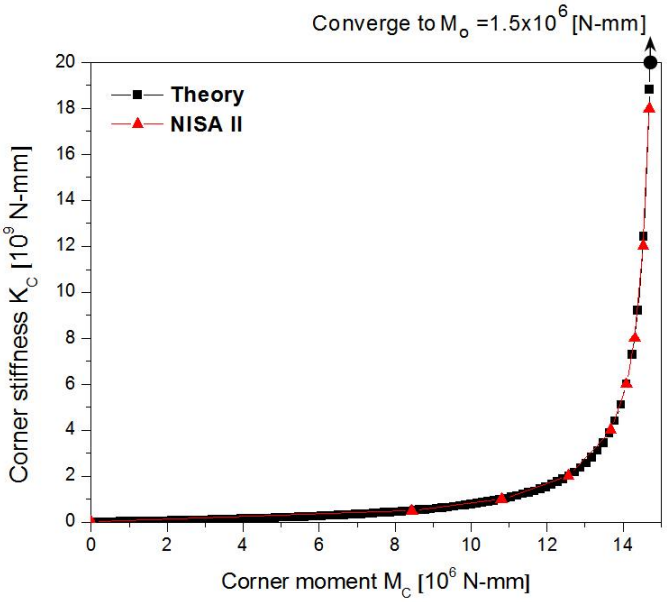

Fig. 8 Relationship between the corner stiffness K_C and corner moment M_C

4. Master curves for the empirical corner stiffness and application to design equation set II

In the previous chapter, design equation set I was derived based on the assumption of a rigid corner. As an extension, design equation set II was derived based on the assumption of finite corner stiffness. For a correct evaluation of the design moments, the correct corner moment is needed. Therefore, an evaluation of the correct corner stiffness is crucial.

The primary problem raised above is resolved for two types of cross-section; rectangular and wide flange beam. The simple approach is as follows. First, compare the bending stresses using design equation set I and FEA. From the error, evaluate reversely the required finite corner stiffness that can nullify the errors for the different dimensions of the cross-section for a given type. These so many empirically obtained corner stiffness can be arranged as a function of the slenderness ratio to be represented by a single master curve.

4.1 Master curve for the right-angle frame of rectangular cross-section

The bending stresses at point A of Fig. 9 for the 18 conditions given in Table 2, were calculated using design equation set I of the rigid corner stiffness. These stresses were compared with the FEA. Fig. 10 shows the difference between the theoretical stresses and the results of FEA according to the slenderness ratio. A small difference in the stress results in for a beam of large slenderness ratio. On the other hand, for a smaller slenderness ratio of the beam, a big difference (> 10%) was shown. In other words, Eq. (18) can be used with a slenderness ratio > 50 but the error is significant for a slenderness ratio < 50. Fig. 11 shows the value of

dimensionless $\tilde{K}_C$ according to the slenderness ratio. This master curve was obtained by the reverse computation to nullify the errors in Fig. 10.

Table 2 Rectangular beam samples [mm]

Type	a	b
S_1	80	25
S_2	90	22
S_3	100	20
	L=H=500, 1000, 1500, 2000, 2500, 3000 P=0.7MPa, E=207GPa	

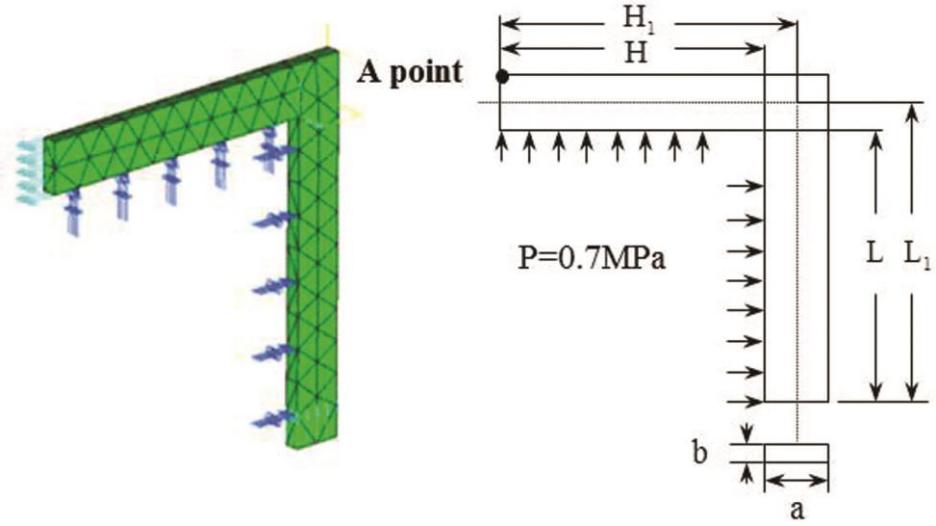

Fig. 9 Boundary conditions and schematic diagram of a horizontal girder with rectangular cross-section

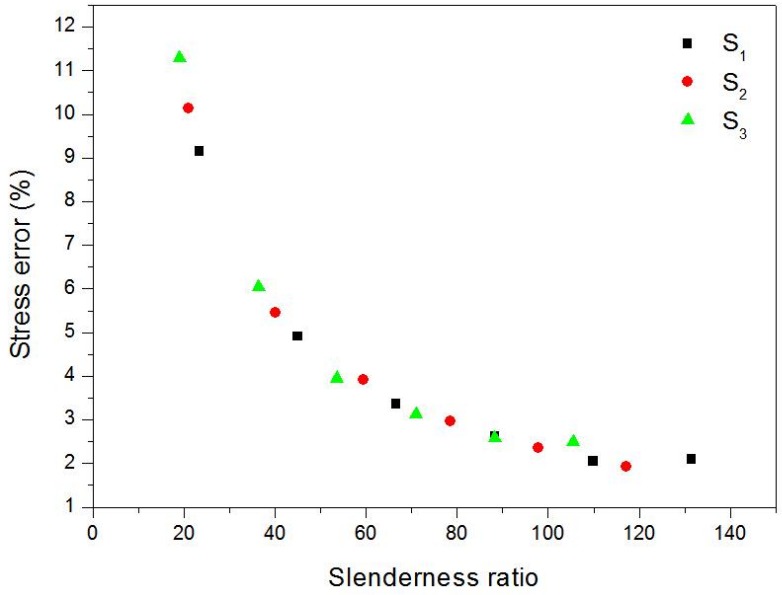

Fig. 10 Error between the theoretical stress (point A) assuming rigid corner stiffness and FEA versus slenderness ratio of the beams with rectangular cross-section

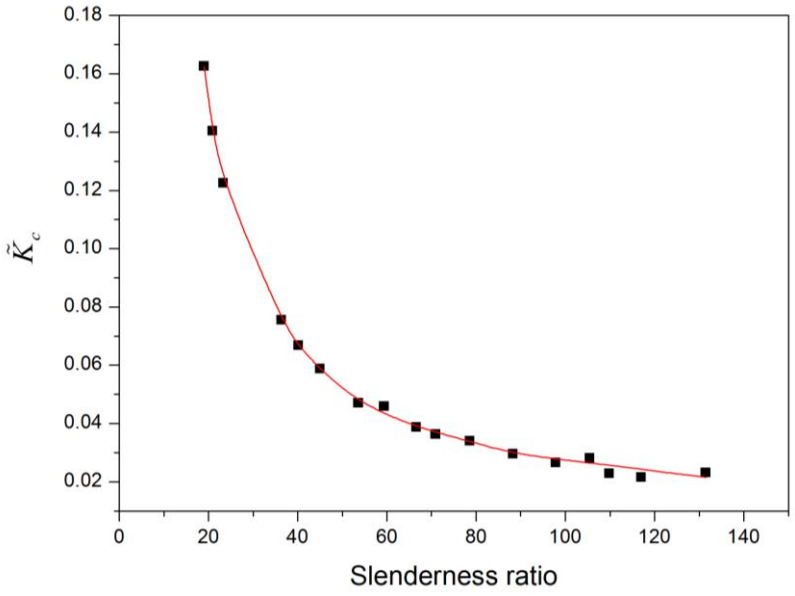

Fig. 11 Master curve for $\tilde{K}_C$ versus the slenderness ratio of the beams with rectangular cross-section

When the slenderness ratio and geometric data are given, the empirical dimensionless corner stiffness was read from the master curve of Fig. 11. With this dimensionless stiffness, the corner moment could be evaluated using Eq. (23).

$$\tilde{K}_C = \frac{K}{K_C} = \frac{EI}{\ell K_C} \tag{24}$$

K_C = stiffness at the corner
K = stiffness for the beam
E = Young's modulus
I = moment of inertia of the section
ℓ = length of the beam to measure

$$M_C = \frac{Q_H(L_1^3 + H_1^3)}{3[(L_1 + H_1) + \ell \tilde{K}_C]} \tag{25}$$

The design moments could be calculated using design equation set II, and Eq. (23) to compute the bending stresses at the centers of the right frame of the rectangular cross-section. The overall procedure is given as follows.

- Evaluate frame properties.
  - Area: A
  - Moment of inertia: I
  - Radius of gyration: κ
  - Slenderness ratio: $\lambda = \ell / k$
  - Read the stiffness ratio $\tilde{K}_C$ from the master curve for the given slenderness ratio λ.
- Calculate the corner moment, M_C, for a given load using the stiffness ratio, $\tilde{K}_C$.
- Calculate the center moments M_{1max} and M_{2max} using the corner moment M_C.
- Calculate the bending stresses at the girder centers using M_{1max} and M_{2max} to check the safety factors.

4.2 Master curve for the right-angle frame of wide flange beam

Before the master curve can be obtained for the right-angle frame of a wide flange beam, the errors between design equation set I and FEA were first calculated for the different web size in sec. 4.2.1 and for the different flange size in sec. 4.2.2.

4.2.1 Comparison of the results between design equation set I and FEA for different web lengths of wide flange beam

The bending stresses at point A of Fig. 12 for the 18 conditions given in Table 3 were calculated using design equation set I of rigid corner stiffness. These stresses were compared with FEA. Fig. 13 shows the difference between the theoretical

stresses and the results of FEA according to the slenderness ratio. The errors in bending stresses large regardless of the slenderness ratio. In other words, a design based on the assumption of rigid corner stiffness might result in an error of more than 15%.

Table 3 Wide flange beam samples of different lengths of web [mm]

Type	A	$B_1 = B_2$	T_1	T_2
S_1	200	200	8	12
S_2	300	200	8	12
S_3	400	200	8	12
		L=H=500, 1000, 1500, 2000, 2500, 3000 P=0.7MPa, E=207GPa		

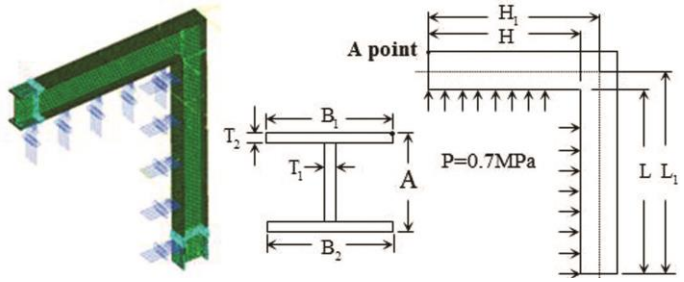

Fig. 12 Boundary conditions and schematic diagram of the wide flange beam model of variable size of web A

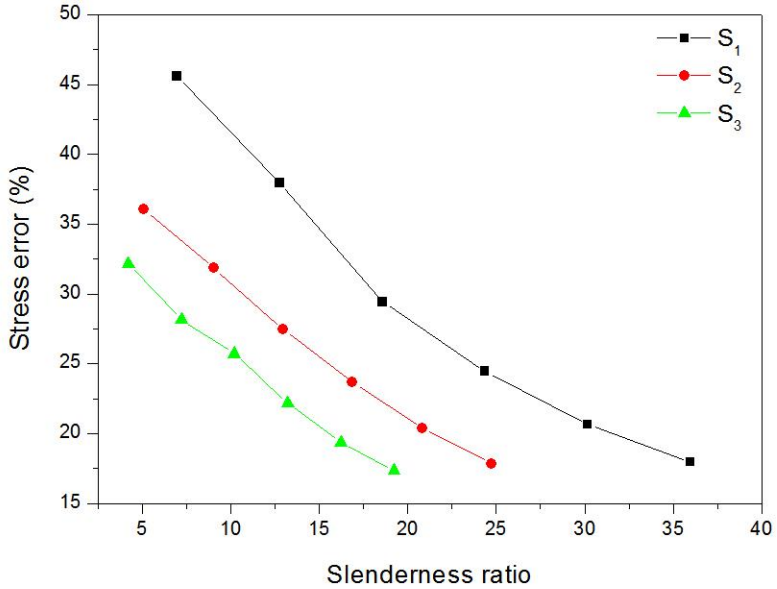

Fig. 13 Error between the theoretical center stress (Point A), assuming rigid corner stiffness, and FEA as a function of the slenderness ratio of a wide flange beams for different lengths of web, A

4.2.2 Comparison of the results between design equation set I and FEA for different flange lengths of wide flange beam

The bending stresses at point A of Fig. 12 for the 24 conditions given in Table 4 were calculated using design equation set I of the rigid corner stiffness. These stresses were compared with FEA in Fig. 15. Fig. 15 shows the difference between the theoretical stresses and the results of FEA according to the slenderness ratio. The errors in the bending stresses were considerable regardless of the slenderness ratio. In other words, a design based on the assumption of rigid corner stiffness might result in an error of more than 10% in most cases. Fig. 16 shows the value of the dimensionless $\tilde{K}_C$ according to the slenderness ratio. This master curve was obtained by reverse computation to nullify the errors in Figs. 13 and 15.

Table 4 Wide flange beam samples as the upper flange variation [mm]

Type	A	B_1	B_2	T_1	T_2
S_4	200	200	200	8	12
S_5	200	150	200	8	12
S_6	200	100	200	8	12
S_7	200	50	200	8	12

L=H=500, 1000, 1500, 2000, 2500, 3000:
P=0.7MPa, E=207GPa

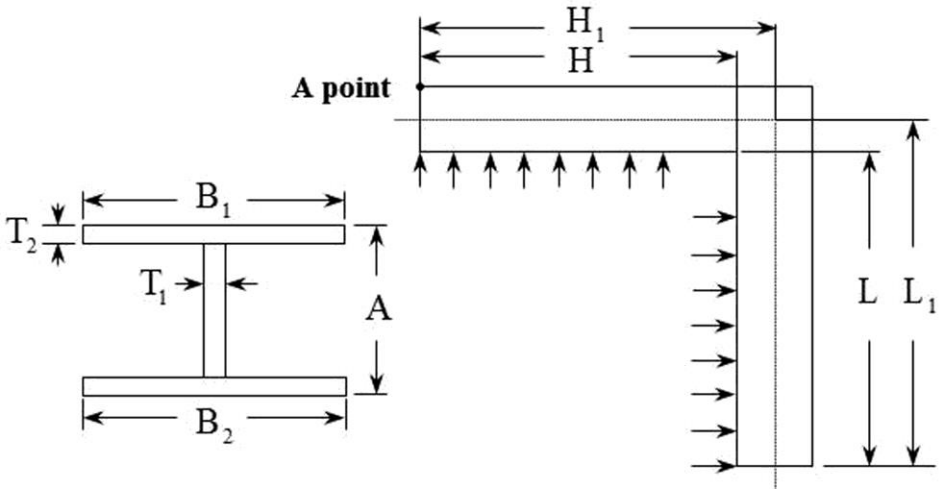

Fig. 14 Schematic diagram of the wide flange beam model of variable size of upper flange B_1

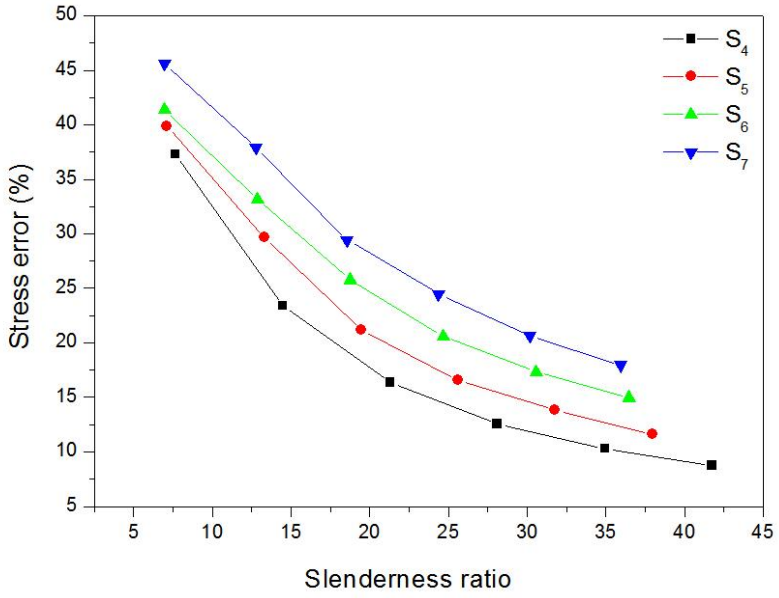

Fig. 15 Error between the theoretical center stress (point A) assuming rigid corner stiffness and FEA as a function of the slenderness ratio of wide flange beam for different lengths of upper flange, B_1

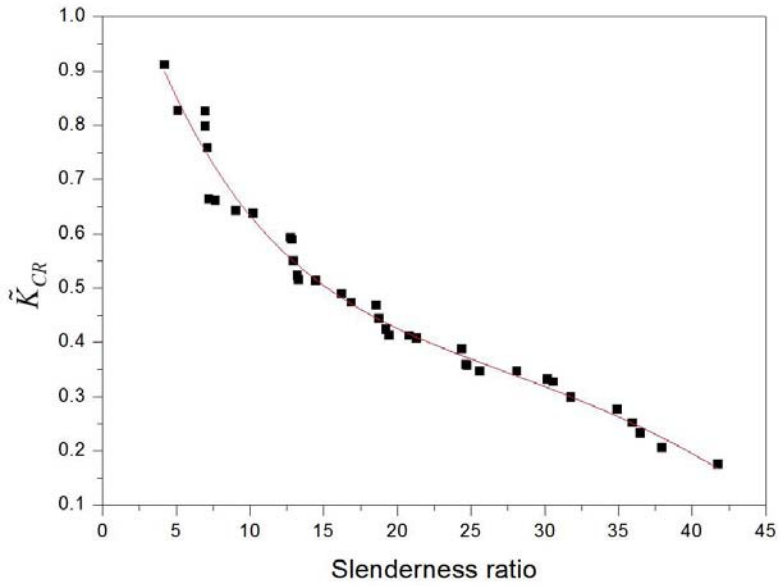

Fig. 16 Master curve for $\tilde{K}_{CR}$ versus slenderness ratio of wide flange beam

When the slenderness ratio and geometric data are given, the empirical dimensionless corner stiffness is read from the master curve of Fig. 16. With this dimensionless stiffness, the corner moment can be evaluated using Eq. (23). The

design moments can be evaluated using design equation set II and Eq. (23) to calculate the bending stresses at the centers of the right frame of the wide flange beam. The overall procedure is the same as that given above for the case of a rectangular cross-section.

4.2.3 Example of using the $\tilde{K}_{CW}$ table of wide flange beam

A structure that is composed of a wide flange beam and loaded by an inner pressure of 0.7 MPa was considered to test the validity of the master curve of Fig. 16. Fig. 17 shows the geometric data of the structure and boundary conditions. Using design equation set I, the corner stress for the wide flange beam was 265MPa. By using the master curve and design equation set II, the corner stress was 216MPa. The reference stress of FEA in Fig. 18 was 214MPa.

The error of 23% in the former theoretical method could be reduced significantly to 0.95% using design equation set II, which is based on the assumption of finite corner stiffness, and the master curve for the empirical corner stiffness.

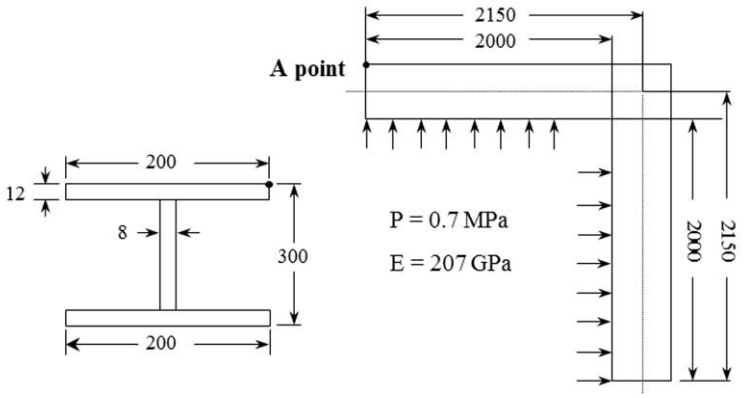

Fig. 17 Schematic diagram of an wide flange beam example

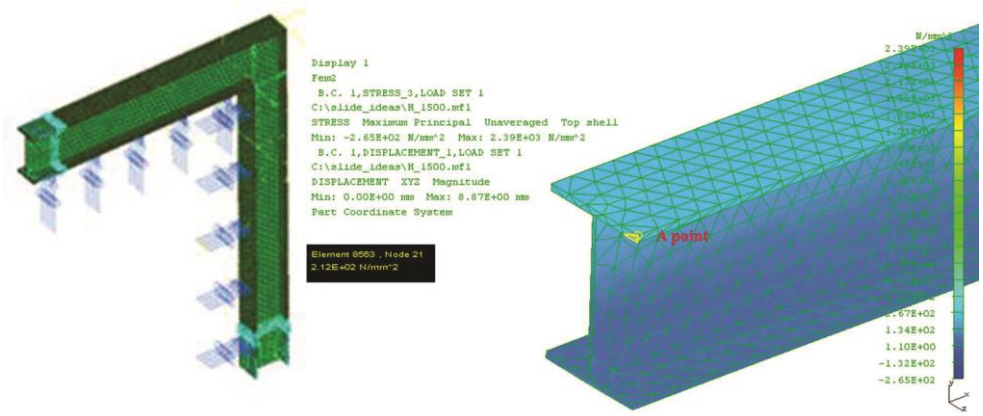

Fig. 18 Boundary conditions of the model and the result at point A

Conclusion

Up to now, the stiffness of the corner of a right-angle frame has been assumed to be infinite. This assumption, however, leads to a considerable or sometimes large error. Two master curves for the dimensionless corner stiffness were obtained by comparing the stresses using derived corner moment for rigid stiffness and FEA. Very accurate design moments and bending stresses of the right-angle frame can be evaluated by applying the empirical corner stiffness to the referred design equation set II. The conclusions of this study are summarized as follows:

- A master curve for the dimensionless corner stiffness was obtained for the right-angle frame of a rectangular cross-section. This can be used to evaluate the corner moment based on the assumption of finite corner stiffness, and to evaluate more accurate design moments and stresses of the right frames.
- A master curve for the right-angle frame of wide flange beam was obtained. This can be used to evaluate the corner and design moments of various dimensions of wide flange beams to analyze and design the right frames more accurately.
- For the right frame of a rectangular cross-section with a slenderness ratio over 50, design equation set I can be used without considerable error. On the other hand, the assumption of rigid corner stiffness leads to significant error for a rectangular cross-section with a slenderness ratio less than 50, and in most cases of a wide flange beam. Therefore, the use of master curves is strongly recommended.

References

Journal articles:

Kwon, Y.-D., Kwon, S.-B., Goo, N.-S. and Jin, S.-B. (2000), “Optimal location of support point for weight minimization in radial gate of dam structure” *Trans. of the KSME(A)*, Vol. **2**(1), 492~497.

Kwon, Y.-D., Jin, S.-B. and Kim, J.-Y. (2004), “Local zooming genetic algorithm and its application to radial gate support problems”, *Structural Engineering Mechanics*, Vol. **17**(5), 611-626.

Kwon, Y.-D., Kwon, S.-B., Gil, H.-M. and Lu, X.-Z. (2013), “Analysis of the right-angle frame with round corner considering a finite corner stiffness”, *Transaction of ASME*, to be submitted

Orbanich, C.J. and Ortega, N.F. (2013), "Analysis of elastic foundation plates with internal and perimetric stiffening beams on elastic foundations by using finite differences method", *Structural Engineering & Mechanics,* **45**(2), 169-182.

Shariatmadar, H. (2011), "Dam-reservoir-foundation interaction effects on the modal characteristic of concrete gravity dams", *Structural Engineering and Mechanics,* **38**(1)**,** 65-79.

Books:
Hydraulic Gate and Penstock Association. (1986), *Technical Standards for Gates and Penstock*.
DIN 19704. (1976), *Hydraulic Steel Structures Criteria for Design and Calculation*.
EMRC. (1994), *NISA II - User's manual*.
Lewin, J. (1995), *Hydraulic gates and valves*, Thomas Telford, London.
Reismann, H. and Pawlik, P. S. (1980), *Elasticity- theory and applications*, John Wiley & Sons, Inc.
Timoshenko, S. P., and Goodier, J. N. (1987), *Theory of Elasticity*, 3rd ed., McGraw-Hill, New York.
Ugural, A.C., and Fenster, S.K. (2003), *Advanced Strength and Applied Elasticity*, 4th ed., Prentice Hall, London.